

## TNF- $\alpha$ signaling drives myeloid skewing and clonal expansion of stem and progenitors in *RUNX1*-familial platelet disorder

by Mona Mohammadhosseini, Aishwarya Sahasrabudhe, Luiza H. Ostrowski, John McClatchy, Rebekah Knight, Kathryn Schabel, Ryland Kagan, Erica Bresciani, Paul Liu and Anupriya Agarwal

Received: July 10, 2025.

Accepted: October 24, 2025.

Citation: Mona Mohammadhosseini, Aishwarya Sahasrabudhe, Luiza H. Ostrowski, John McClatchy, Rebekah Knight, Kathryn Schabel, Ryland Kagan, Erica Bresciani, Paul Liu and Anupriya Agarwal.

TNF- $\alpha$  signaling drives myeloid skewing and clonal expansion of stem and progenitors in *RUNX1*-familial platelet disorder.

Haematologica. 2025 Nov 6. doi: 10.3324/haematol.2025.288410 [Epub ahead of print]

### *Publisher's Disclaimer.*

E-publishing ahead of print is increasingly important for the rapid dissemination of science.

Haematologica is, therefore, E-publishing PDF files of an early version of manuscripts that have completed a regular peer review and have been accepted for publication.

E-publishing of this PDF file has been approved by the authors.

After having E-published Ahead of Print, manuscripts will then undergo technical and English editing, typesetting, proof correction and be presented for the authors' final approval; the final version of the manuscript will then appear in a regular issue of the journal.

All legal disclaimers that apply to the journal also pertain to this production process.

# **TNF- $\alpha$ signaling drives myeloid skewing and clonal expansion of stem and progenitors in RUNX1-familial platelet disorder**

**Running Title:** *Inhibiting TNF- $\alpha$  Reverses Myeloid Skewing in FPD*

**Authors:** Mona Mohammadhosseini<sup>1,2,3,4\*</sup>, Aishwarya Sahasrabudhe<sup>1,2,3,4\*</sup>, Luiza H. Ostrowski<sup>1,2,3,4</sup>, John McClatchy<sup>1,2,3,4</sup>, Rebekah Knight<sup>5</sup>, Kathryn Schabel<sup>6</sup>, Ryland Kagan<sup>6</sup>, Erica Bresciani<sup>7</sup>, Paul Liu<sup>7</sup>, and Anupriya Agarwal<sup>1,2,3,4</sup>.

**\* Equal contribution authors**

<sup>1</sup>The Knight Cancer Institute, Oregon Health and Science University, Portland, OR, USA

<sup>2</sup> Division of Oncological Sciences, Oregon Health and Science University, Portland, OR, USA

<sup>3</sup> Department of Cell, Developmental, and Cancer Biology, Oregon Health & Science University, Portland, OR, USA

<sup>4</sup> Department of Molecular and Medical Genetics, Oregon Health & Science University, Portland, OR, USA

<sup>5</sup> Cellular Therapy Laboratory, Oregon Health and Science University, Portland, OR, USA

<sup>6</sup> Department of Orthopedics & Rehabilitation, Oregon Health and Science University, Portland, OR, USA

<sup>7</sup> Oncogenesis and Development Section, Division of Intramural Research, National Human Genome Research Institute, NIH, Bethesda, MD, USA

**Corresponding Author's Email Address:** Anupriya Agarwal [agarwala@ohsu.edu](mailto:agarwala@ohsu.edu)

**Key words:** RUNX1, FPD, TNF- $\alpha$ , hematopoiesis, etanercept

## **Acknowledgments**

We thank OHSU Massively Parallel Sequencing Shared Resource, Flow Cytometry, and Knight Biorepository, as well as the OHSU Department of Comparative Medicine, for support. We thank Hsin-Yun Lin for providing the guidance in performing some experiments.

## **Funding**

Funding for this project was provided by the Edward P. Evans Foundation and *the RUNX1* Research Program (A.A.); the Chan Zuckerberg Initiative (A.A.), the National Heart, Lung, and Blood Institute (R01 HL155426-01: A.A.); and the National Cancer Institute (U01 CA257666: A.A.). A.A. is also supported by grants from the Alex Lemonade Stand Foundation and RUNX1 Research Program, the National Cancer Institute (U01 CA229875), the National Cancer Institute (U54 CA224019) as well as the Knight Cancer Research Institute pilot research projects and exploratory seed grant, and by a. M. M. is supported by institutional T32 (T32CA254888); OHSU Covid Research funds; and National Heart, Lung, and Blood Institute NRSA F31 (F31HL162542). L.H.O. is supported by ARC under award number S10OD034224. The FPD sample collection was partly supported by the Intramural Research Programs of the National Human Genome Research Institute (E.B. and P.L.).

## **Authorship Contribution**

A.A. provided project oversight for experimental design, data analysis, interpretation, methods development, and resources. M. M. designed and performed most of the experiments, analyzed the data, and was supported by A.A. and A.S. for the experiments. M. M., and A.S. performed single-cell and bulk-sequencing experiments. L.H.O. and M.M. performed transcriptomic analyses. J.M. contributed to the development of the murine model. R. Knight, K.S., R. Kagan, E.B., and P.L. provided critical resources and guidance for patient samples. All the authors wrote or edited the manuscripts, provided feedback, and agreed to submit the manuscript.

## **Disclosure of Conflicts of Interest**

The other authors declare that they have no competing interests.

## **Data Sharing Statement**

The data that support the findings of this study are available as a supplementary file and can be requested from the corresponding author.

### ***Letters to the Editor:***

*RUNX1*-Familial platelet disorder (FPD) is an autosomal dominant disease caused by germline *RUNX1* loss-of-function mutations. *RUNX1*-FPD is one of the most common inherited forms of myeloid malignancies<sup>1</sup>. Over 250 families in the U.S. have been identified, and a recent estimate indicates that ~18,000 patients exist<sup>2</sup>. *RUNX1*-FPD patients suffer from platelet dysfunction, thrombocytopenia, and increased inflammatory diseases, and about 40-50% of the patients have a lifelong risk of developing hematological malignancies, especially myelodysplastic syndromes (MDS) and acute myeloid leukemia (AML), with a median onset age of 29 years (range 6-76 years)<sup>3</sup>. Currently, there is a lack of early intervention or prevention strategies for *RUNX1*-FPD patients from developing hematological malignancies.

Recently, we and others identified that the *RUNX1*-FPD bone marrow microenvironment is highly inflammatory, and many inflammatory pathways, including TNF- $\alpha$  signaling, are significantly enriched in *RUNX1*-FPD HSPCs compared to healthy controls<sup>4-6</sup>. However, the role of TNF- $\alpha$  signaling in *RUNX1*-FPD hematopoiesis and evolution has not been fully demonstrated. Previous studies have shown that TNF- $\alpha$  is implicated in cytotoxicity against tumor cells, immunomodulation, and inflammatory responses. TNF- $\alpha$  is primarily produced by immune cells, such as macrophages and T-cells, and leukemia stem cells to promote cell survival and treatment resistance. TNF- $\alpha$  upregulation drives leukemia transformation from a pre-malignant state, as demonstrated in both *in vivo* and *in vitro* models using *Dnmt3A*<sup>R882/+</sup> and the Fanconi anemia mouse model<sup>7,8</sup>. TNF- $\alpha$  antagonists are approved for treating autoimmune diseases effectively, but have not yet been examined as early intervention strategies in AML. In this study, we demonstrate that TNF- $\alpha$  drives resistance to inflammatory stress-mediated exhaustion, characterized by an increased myeloid bias of *RUNX1*-FPD progenitors, compared to healthy controls, through transcriptomic and epigenetic mechanisms. Furthermore, inhibition of TNF- $\alpha$  signaling in *RUNX1*-FPD rescues the differentiation defects of progenitors in murine models and human cells.

Specifically, we utilized *RUNX1*-FPD bone marrow samples from the pre-leukemia stage, obtained from the NIH (NCT03854318), as approved by the Institutional Review Board. Mononuclear cells (MNCs) and CD34<sup>+</sup> progenitors were purified. Healthy bone marrow samples

were age- and gender-matched to serve as controls (**Table S1**). The pathway enrichment analysis of upregulated genes from published scRNA-seq data reveals enrichment of TNF- $\alpha$  signaling in *RUNX1*-FPD compared to controls (**Figure 1A**)<sup>4</sup>. We validated these results using bulk RNA-sequencing on *RUNX1*-FPD and healthy CD34<sup>+</sup> progenitors (**Figure 1B**). Differentially expressed genes (DEG) in *RUNX1*-FPD showed upregulation of inflammatory pathways, including TNF- $\alpha$  signaling (**Figure 1C-D**) and RELA transcription factor, a mediator of TNF- $\alpha$  signaling (**Figure 1E**). The expression of TNF- $\alpha$  receptors is significantly upregulated for TNFR2 (TNFRSF1B) but not TNFR1 (TNFRSF1A) in *RUNX1*-FPD HSPCs compared to healthy controls (**Figure 1F**). Previous cytokine analysis<sup>4</sup> of the BM extracellular fluid in FPD also showed elevated levels of TNF- $\alpha$  and soluble TNF-RII receptor (**Figure 1G**). Consistent with *RUNX1*-FPD patients, TNFR2 (TNFRSF1B), but not TNFR1 (TNFRSF1A), was also upregulated in *RUNX1*-mutated AML patient samples compared to *RUNX1*-wild type samples (**Figure S1A-B**). To identify the impact of TNF- $\alpha$  on *RUNX1*-FPD HSPC growth and differentiation, we performed a colony formation assay using primary BM CD34<sup>+</sup> progenitors derived from *RUNX1*-FPD and healthy individuals. We demonstrated that *RUNX1*-FPD HSPCs have significantly more colony formation ability compared to healthy HSPCs. Both *RUNX1*-FPD and healthy HSPCs exhibited slight growth suppression upon TNF- $\alpha$  stimulation (**Figure 1H**), suggesting TNF- $\alpha$  may be cytotoxic to progenitors. However, *RUNX1*-FPD maintained an increased myeloid bias (CFU-GM) under TNF- $\alpha$ -mediated inflammatory stress. Overall, these results show that the upregulated TNF- $\alpha$  signaling enhanced the myeloid bias of *RUNX1*-FPD HSPCs (**Figure 1H**).

To understand how TNF- $\alpha$  is impacting myeloid bias in *RUNX1*-FPD bone marrow cells, we performed 10X single-cell RNA sequencing using *RUNX1*-FPD mononuclear cells (MNCs) (n = 2) treated with TNF- $\alpha$  and its inhibitor, etanercept. We identified 11 cell clusters across the vehicle and treated samples (**Figure S2A**). Exposure of bone marrow cells with TNF- $\alpha$  resulted in the expansion of the monocytic-macrophage (Mono/Mac), HSCs, and progenitor populations (HSC/progenitors, >1.7-fold) while suppressing T-cells by 2-fold (**Figure 2A**). However, etanercept treatment did not impact HSC/progenitors while slightly suppressing Mono/Mac populations. The GSEA pathway analysis of DEGs in the HSC/progenitors showed that TNF- $\alpha$  exposure led to the upregulation of inflammatory response pathways and TNF- $\alpha$  signaling, and etanercept treatment led to its suppression compared to vehicle-treated *RUNX1*-FPD cells

(Figure 2B). In addition, TNF- $\alpha$  upregulated mTOR and IL-6/JAK/STAT3 pathways, and etanercept treatment inhibited these pathways, suggesting that etanercept can suppress increased inflammation and mTOR and JAK/STAT signaling. Recently, we demonstrated that FPD HSPCs exhibit a differentiation bias towards myeloid cells and fewer megakaryocytes, resulting from the upregulation of CD74-mediated inflammation via PI3K/mTOR and JAK/STAT signaling<sup>4</sup>. Activation of the CD74 pathway was shown to induce expression and secretion of TNF- $\alpha$ <sup>9</sup>. Further, TNF- $\alpha$ -dependent inflammation contributed to the progression of lung adenocarcinoma by upregulating MIF/CD74 in a positive feedback loop<sup>10</sup>, suggesting TNF- $\alpha$  could also be part of the CD74 axis. Our data also suggest that increased TNF- $\alpha$  promotes cytotoxicity in progenitors by increasing oxidative phosphorylation, reactive oxygen species, and DNA damage pathways, leading to increased apoptosis, which we also found to be upregulated in GSEA analyses. Etanercept reverses these effects, suggesting that it may improve stem cell functions by enhancing their tolerance to inflammatory stress. Overall, these results show that TNF- $\alpha$  signaling promotes myeloid cell expansion in *RUNX1*-FPD, and etanercept treatment rescues these effects.

Next, we evaluated how TNF- $\alpha$  signaling is upregulated in *RUNX1*-FPD. Our bulk RNAseq analysis shows enrichment of the RELA transcription factor in *RUNX1*-FPD (Figure 1E). Thus, we utilized a publicly available ChIP-Seq dataset to investigate the extent of RELA binding at the transcription start site (TSS) of TNF- $\alpha$  and its receptors. We observed that RELA binding is enhanced in the monocytic AML cell line (THP1) at the TNF- $\alpha$  gene, compared to the non-monocytic cell line (K562), and RELA binding on TNF- $\alpha$  and TNF receptors is stronger with TNF- $\alpha$  treatment in the non-monocytic cell line (Figure 2C). To understand the effect of TNF- $\alpha$  on chromatin accessibility, we performed 10X single-cell ATAC sequencing on healthy and FPD MNCs. We observed that RELA TSS is more accessible in *RUNX1*-FPD compared to healthy controls. Interestingly, RELA accessibility in the monocyte population increases with TNF- $\alpha$  stimulation and decreases with etanercept, indicating that high TNF- $\alpha$  in *RUNX1*-FPD enhances chromatin accessibility at the TSS of the RELA, which may upregulate TNF- $\alpha$  signaling through a positive feedback mechanism (Figure 2D).

TNF- $\alpha$  signaling inhibitor etanercept is approved for treating patients with rheumatoid arthritis and psoriasis<sup>11</sup>. Since TNF- $\alpha$  is a major driver of inflammation, it could be an attractive approach

in leukemia treatment and should be further evaluated<sup>7</sup>. To determine the impact of etanercept on the function of *RUNX1*-FPD progenitors, first, we evaluated its effect on the viability of *RUNX1*-FPD bone marrow cells using an *in vitro* concentration gradient (**Figure S2B**). *RUNX1*-FPD and healthy bone marrow cells maintained a viability of greater than 90% for the etanercept dose curve tested. Next, we quantified the effect of etanercept on *RUNX1*-FPD MNCs on the differentiation of myeloid and megakaryocytes. We showed a significant decrease in monocyte (CD14<sup>+</sup>/13<sup>+</sup>) and an increase in megakaryocyte (CD41<sup>+</sup>/61<sup>+</sup>) cell populations (**Figure 3A**). Etanercept also decreased levels of CCL24, CXCL8, and M-CSF cytokines (**Figure S2C**). The treatment of *RUNX1*-FPD bone marrow cells with etanercept also reduced the phosphorylation of proteins involved in PI3K/mTOR and NF-κB signaling, including p65, AKT, SRC, S6, and 4EBP1 (**Figure 3B**), validating the RNA-seq analysis (**Figure 2B**). Additionally, etanercept resulted in a significant reduction in colony formation ability in *RUNX1*-FPD with minimal impact on healthy controls (**Figure 3C, S2D**).

Often, the transition of *RUNX1*-FPD to leukemia is accompanied by an intermediate stage of clonal hematopoiesis (CH) due to the acquisition of somatic mutations in genes such as *TET2*. An estimated 10-22% of *RUNX1*-FPD patients have *TET2* mutations<sup>12</sup>. *TET2* loss-of-function mutations are commonly found in CH, MDS, and AML and are associated with a poor prognosis<sup>13</sup>. *TET2*-mutated HSPCs have been shown to have an advantage in expansion with myeloid skewing and resistance to apoptosis in the presence of chronic TNF-α<sup>14</sup>. Additionally, increased TNF-α levels in aged *Tet2*<sup>-/-</sup> mice led to the expansion of HSCs and myeloid skewing<sup>15</sup>. Thus, we tested the effect of etanercept on the expansion of *TET2*-mutated cells. For this, we CRISPR-edited *TET2* in *RUNX1*-FPD HSPCs and performed a colony formation assay. *TET2* editing in *RUNX1*-FPD progenitors caused a slight increase in the colony formation ability of *RUNX1*-FPD compared to non-targeting control (**Figure 3D**). Etanercept significantly reduced the colony formation ability of *TET2*-edited *RUNX1*-FPD cells, a reduction that is more pronounced compared to non-*TET2*-edited *RUNX1*-FPD progenitors. We used murine progenitors harboring a heterozygous germline *Runx1* mutation (R188Q) and a heterozygous deletion of *Tet2* (*Runx1*<sup>Mut</sup>/*Tet2*<sup>Het</sup>). These experiments were conducted in accordance with the OHSU Institutional Animal Care and Use Committee guidelines. We found that etanercept significantly suppressed colony growth in both *Runx1*<sup>Mut</sup> and *Runx1*<sup>Mut</sup>/*Tet2*<sup>Het</sup> progenitors (**Figure 3E**). These results demonstrate the effectiveness of etanercept in inhibiting the growth of

*RUNX1*-FPD HSPCs with *TET2* loss-of-function mutations. Since MIF/CD74 inhibitors are not currently accessible clinically, exploring the repurposing of etanercept to inhibit TNF- $\alpha$  signaling as a potential approach may increase *RUNX1*-FPD megakaryocytic differentiation while suppressing myelopoiesis.



## **References**

1. Rio-Machin A, Vulliamy T, Hug N, et al. The complex genetic landscape of familial MDS and AML reveals pathogenic germline variants. *Nat Commun.* 2020;11(1):1044.
2. Luo X, Feurstein S, Mohan S, et al. ClinGen Myeloid Malignancy Variant Curation Expert Panel recommendations for germline RUNX1 variants. *Blood Adv.* 2019;3(20):2962-2979.
3. West AH, Godley LA, Churpek JE. Familial myelodysplastic syndrome/acute leukemia syndromes: a review and utility for translational investigations. *Ann N Y Acad Sci.* 2014;1310(1):111-118.
4. Mohammadhosseini M, Enright T, Duvall A, et al. Targeting the CD74 signaling axis suppresses inflammation and rescues defective hematopoiesis in RUNX1-familial platelet disorder. *Sci Transl Med.* 2025;17(780):eadn9832.
5. Ahmad MH, Hedge M, Wong WJ, et al. Runx1-R188Q germline mutation induces inflammation and predisposition to hematologic malignancies in mice. *Blood Adv.* 2023;7(23):7304-7318.
6. Zezulin AU, Yen D, Ye D, et al. RUNX1 is required in granulocyte-monocyte progenitors to attenuate inflammatory cytokine production by neutrophils. *Genes Dev.* 2023;37(13-14):605-620.
7. Verma S, Singh A, Yadav G, et al. Serum Tumor Necrosis Factor-Alpha Levels in Acute Leukemia and Its Prognostic Significance. *Cureus.* 2022;14(5):e24835.
8. SanMiguel JM, Eudy E, Loberg MA, et al. Distinct Tumor Necrosis Factor Alpha Receptors Dictate Stem Cell Fitness versus Lineage Output in Dnmt3a-Mutant Clonal Hematopoiesis. *Cancer Discov.* 2022;12(12):2763-2773.
9. Roger T, Chanson AL, Knaup-Reymond M, Calandra T. Macrophage migration inhibitory factor promotes innate immune responses by suppressing glucocorticoid-induced expression of mitogen-activated protein kinase phosphatase-1. *Eur J Immunol.* 2005;35(12):3405-3413.
10. Cao L, Wang X, Liu X, et al. Tumor Necrosis Factor  $\alpha$ -Dependent Lung Inflammation Promotes the Progression of Lung Adenocarcinoma Originating From Alveolar Type II Cells by Upregulating MIF-CD74. *Lab Invest.* 2023;103(3):100034.
11. Haraoui B, Bykerk V. Etanercept in the treatment of rheumatoid arthritis. *Ther Clin Risk Manag.* 2007;3(1):99-105.
12. Brown AL, Arts P, Carmichael CL, et al. RUNX1-mutated families show phenotype heterogeneity and a somatic mutation profile unique to germline predisposed AML. *Blood Adv.* 2020;4(6):1131-1144.
13. Chou W-C, Chou S-C, Liu C-Y, et al. TET2 mutation is an unfavorable prognostic factor in acute myeloid leukemia patients with intermediate-risk cytogenetics. *Blood.* 2011;118(14):3803-3810.
14. Abegunde SO, Buckstein R, Wells RA, Rauh MJ. An inflammatory environment containing TNF $\alpha$  favors Tet2-mutant clonal hematopoiesis. *Exp Hematol.* 2018;59:60-65.
15. Quin C, DeJong E, McNaughton AJM, et al. Chronic TNF in the Aging Microenvironment Exacerbates TET2-loss-of-Function Myeloid Expansion. *Blood.* 2023;142(Supplement 1):938.

### Figure Legends:

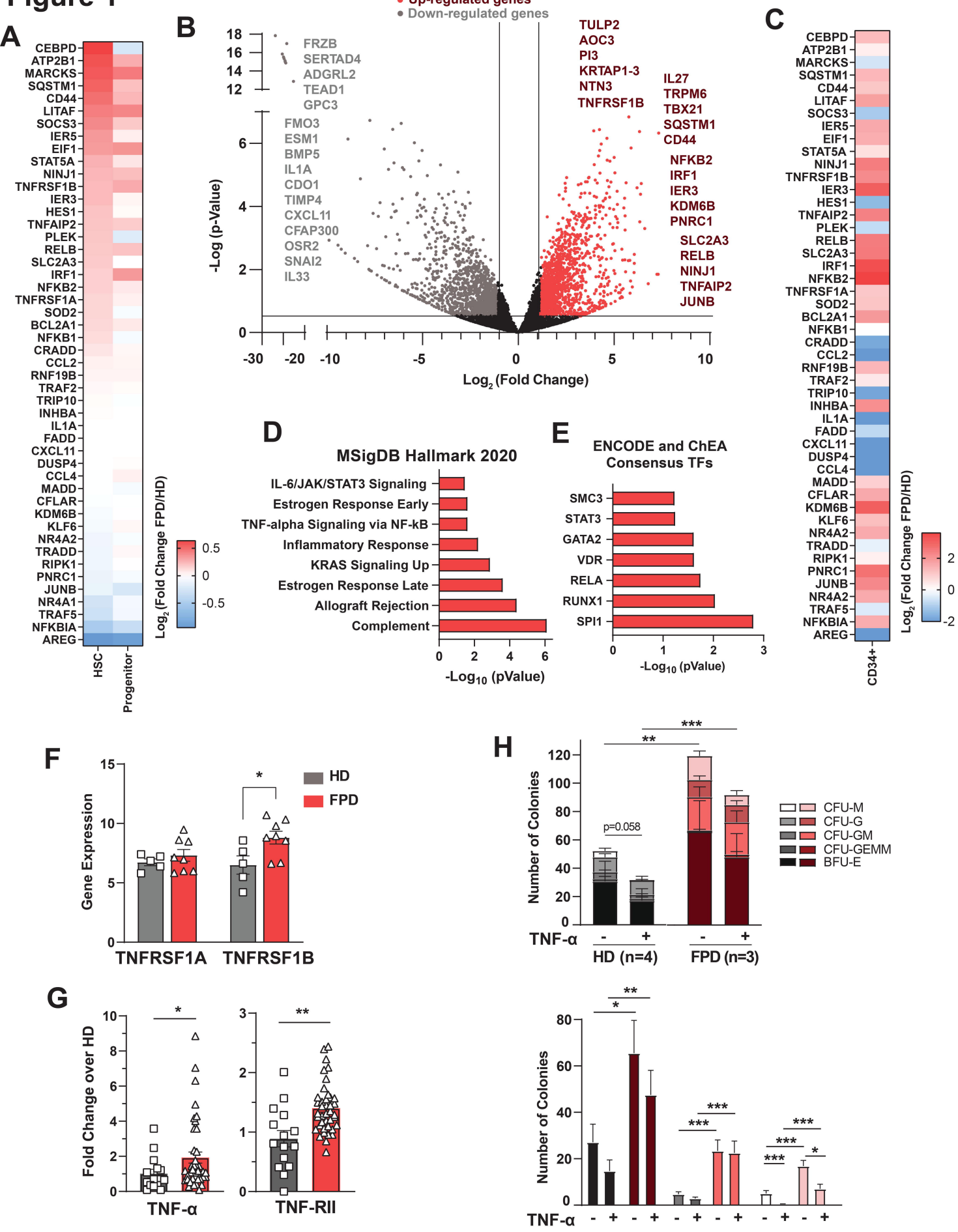
**Figure 1. TNF- $\alpha$  signaling is upregulated in *RUNX1*-FPD compared to healthy controls (HD).** **A)** Differential gene expression between *RUNX1*-FPD (n=10) and HD (n=4) using scRNA-seq analysis. The genes are selected based on published databases for the leading genes in the TNF- $\alpha$  signaling pathway. **B)** The bulk RNA sequencing analysis was performed using purified CD34<sup>+</sup> cells. Volcano plot showing upregulated (red) and downregulated (grey) genes in *RUNX1*-FPD (n=8) over HD (n=5) CD34<sup>+</sup> cells. **C)** Expression of the leading genes in the TNF- $\alpha$  signaling pathway in bulk RNA seq analysis. **D)** Pathway analysis on significantly (p-Adj<0.05) upregulated (>2-fold) genes in *RUNX1*-FPD compared to healthy controls. The analysis was done using the Enrichr database. **E)** Enrichment of transcription factors in upregulated genes (p-Adj<0.05, >2-fold) in *RUNX1*-FPD compared to healthy was assessed using Enrichr database. **F)** Expression of TNF- $\alpha$  receptors is shown using bulk RNA seq analysis of HSPCs. **G)** TNF- $\alpha$  and TNF-RII levels in *RUNX1*-FPD (n=40) bone marrow fluid are compared to HD (n=15) as evaluated using 65-plex luminex assay. The data is presented as fold change over average HD values. **H)** The results of the colony formation ability of *RUNX1*-FPD and HD CD34<sup>+</sup> HSPCs in the presence of TNF- $\alpha$  cytokine. Primary CD34<sup>+</sup> cells were seeded at a density of 1,000 cells/well and treated with TNF- $\alpha$  at 1.0 ng/mL using methocult (*StemCell*, H4434). Colonies were counted on day 14 post-seeding. Statistical significance is calculated using the students' t-test and levels indicating differences between FPD and healthy control samples, or untreated and treated groups, as \* p $\leq$ 0.05, \*\* p $\leq$ 0.01, \*\*\* p $\leq$ 0.001

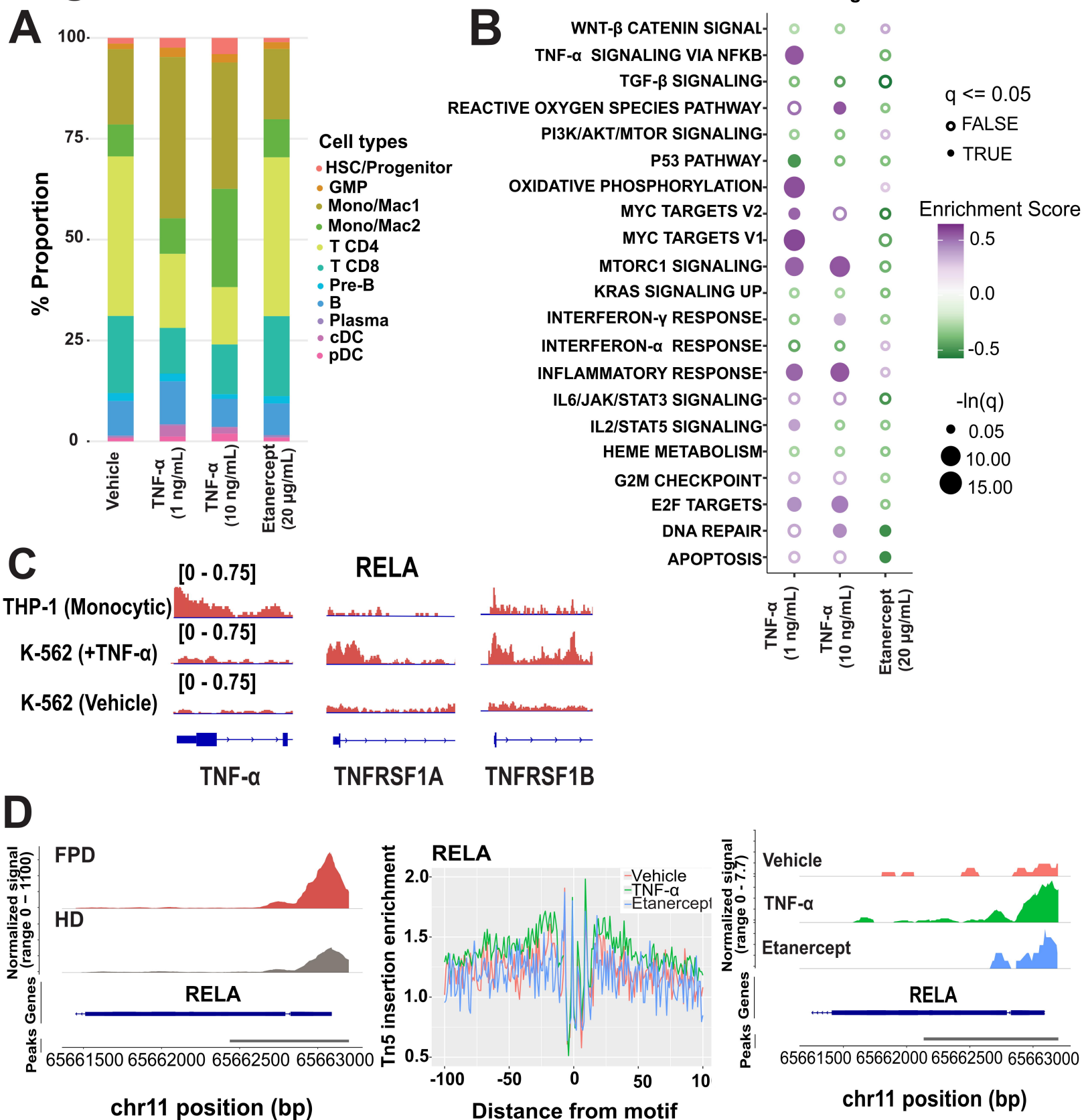
**Figure 2. Single-cell transcriptomic analysis shows the expansion of myeloid cells upon TNF- $\alpha$  treatment in *RUNX1*-FPD.** **A)** *RUNX1*-FPD (n=2) bone marrow cells were treated overnight with TNF- $\alpha$  (1 ng/mL and 10 ng/mL) and etanercept (20  $\mu$ g/mL). Cells were then subjected to 10X Chromium single-cell RNA sequencing. Approximately 2,600 cells were analyzed in the vehicle group, 2,200 cells in the TNF- $\alpha$  (1 ng/mL) group, 1,700 cells in the TNF- $\alpha$  (10 ng/mL) group, and 2,100 cells in the etanercept-treated group. The percentage of each cell population in different treatment groups is shown in bar graphs. **B)** Differential expression analysis of each treatment over vehicle was performed using the FindMarkers function from Seurat and gene set enrichment analysis (GSEA) was performed using the clusterProfiler package (v4.10.1). GSEA analysis of DEGs in each treatment group compared to vehicle-treated cells shows enrichment of different pathways. **C)** RELA binding at the TSS of TNF- $\alpha$ , TNFRSF1A, and TNFRSF1B genes in THP-1 (monocytic, SRX4001967), and K-562 (+TNF- $\alpha$ , SRX14499808; vehicle, SRX2424413) cell lines, plotted from public datasets using ChIP-Atlas (<https://chip-atlas.org/>). **D)** *RUNX1*-FPD bone marrow cells were treated overnight with TNF- $\alpha$  (1 ng/mL) and etanercept (20

μg/mL). Cells were then subjected to 10X single cell ATAC sequencing along with HD bone marrow cells. Coverage plot showing chromatin accessibility on the RELA TSS region in *RUNX1*-FPD and HD monocytes (left). Footprint profile plot of RELA in monocytes. Coverage plot (right) showing normalized signal of open chromatin along the RELA TSS in FPD. Single-cell data is available through the dbGAP accession ID. Phs003508.

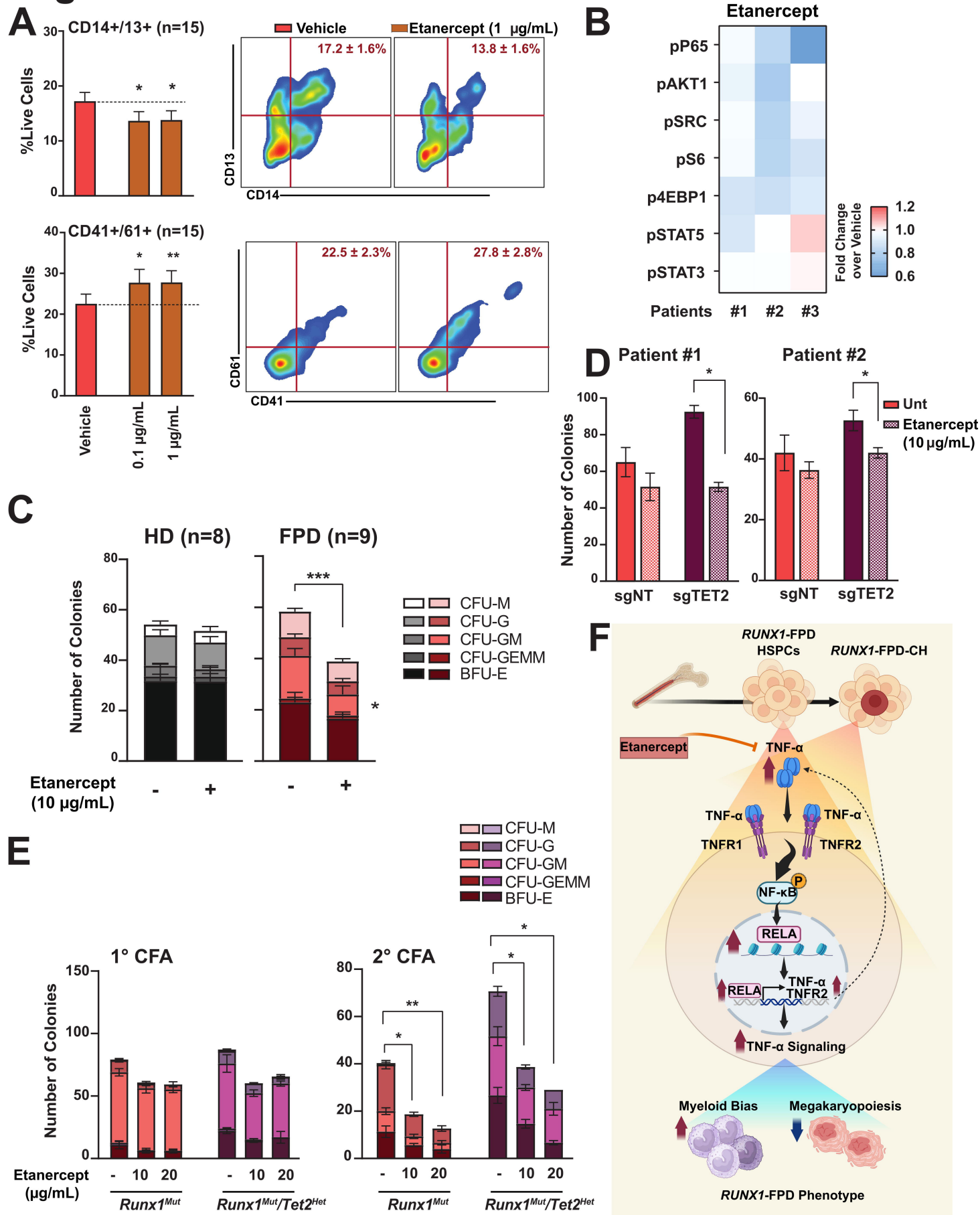
**Figure 3. TNF-α pathway inhibition reverses *RUNX1*-FPD phenotype.** **A)** MNCs were separated from primary *RUNX1*-FPD (n=15) samples and used *in vitro* to culture in the presence of etanercept for 7 days. Cells were collected, and differentiation analysis was done using flow cytometry. The bar graphs show the percentage of live cells in myeloid (CD13<sup>+</sup>/14<sup>+</sup>) and megakaryocytes (CD41<sup>+</sup>/61<sup>+</sup>) populations upon treatment with etanercept at 2 different concentrations. A flow plot representation of bar graphs is shown on the right. **B)** *RUNX1*-FPD MNCs (n=3) were cultured with etanercept (20 μg/mL) for 48 hours, and phosphorylation levels of the indicated proteins were measured through intracellular flow cytometry. **C)** The results of colony formation ability of *RUNX1*-FPD (n=9) and HD (n=8) CD34<sup>+</sup> HSPCs in the presence of TNF-α inhibitor, etanercept. Primary CD34<sup>+</sup> cells were seeded at a density of 1,000 cells/well (in duplicate plating) and treated with etanercept at 10 μg/mL in Methocult (*StemCell*, H4434). Colonies were counted on day 14 post-seeding. **D)** HSPCs enriched from primary FPD (n=2) bone marrow samples were subject to deletion of *TET2* via CRISPR/Cas9 method. The cells were recovered overnight in serum-free media (SEM II, *StemCell*) supplemented with SCF (100ng/mL), TPO (100ng/mL), FLT3-L (100ng/mL), IL-6 (100ng/mL), LDL (10ug/mL), and UM171 (35nM). The results of the colony formation ability using Methocult of *TET2*-edited FPD CD34<sup>+</sup> (n=2, in triplicate plating) treated with etanercept and compared to NT-edited cells are shown in bar graphs. **E)** Heterozygous *Runx1*-knockin mice (R188Q/+, *Runx1*<sup>Mut</sup>) were bred with mice harboring *Tet2*-floxed and *SCL-Cre* (JAX, 037467) alleles. The mice heterozygous for *Runx1* and *Tet2* carrying *SCL-Cre* were selected and treated with tamoxifen to activate *SCL-Cre*. Tamoxifen was dissolved in corn oil at 30 mg/mL concentration, and mice were given a total of 100 mg/kg tamoxifen by oral gavage in 5 consecutive days. Approximately 3 weeks after the treatment, the deletion of the *Tet2*-floxed allele in peripheral blood was confirmed using PCR. Lineage-negative cells from heterozygous *Runx1*-mutated (*Runx1*<sup>Mut</sup>) and heterozygous *Runx1*-mutated with *Tet2* deletion (*Runx1*<sup>Mut</sup>/*Tet2*<sup>Het</sup>) mice were harvested. Cells were used in a colony formation assay using Methocult (*StemCell*, M3434) in the presence of etanercept at two different concentrations. The colonies were counted at 7 days post-seeding and harvested for secondary plating. For primary plating, 3,000 cells/well and for secondary plating, 100k cells/well were used. Statistical significance is calculated using the Student's t-test and levels indicating differences between untreated and treated groups as \* p≤0.05, \*\*

$p \leq 0.01$ , \*\*\*  $p \leq 0.001$ . **F)** Schematic showing TNF- $\alpha$  inhibition by Etanercept reverses myeloid bias and promotes megakaryopoiesis in *RUNX1*-Familial Platelet Disorder in vitro ([BioRender.com/er8qn93](https://BioRender.com/er8qn93)).

**Figure 1**

**Figure 2**

# Figure 3



**TNF- $\alpha$  signaling drives myeloid skewing and clonal expansion of stem and progenitors in *RUNX1*-FPD**

**SUPPLEMENTAL INFORMATION**

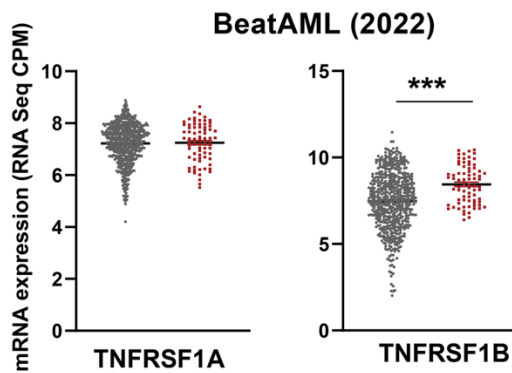
**Supplemental Figures**

- Figure S1. TNFR2 (TNFRSF1B) is upregulated in *RUNX1*-mutated AML samples.
- Figure S2. Etanercept treatment can reverse *RUNX1*-FPD phenotype without causing toxicity.
- Table S1 provided as Excel file. Information on FPD patient samples and HD controls used in the manuscript.



## Supplemental Figure 1

**A**



**B**

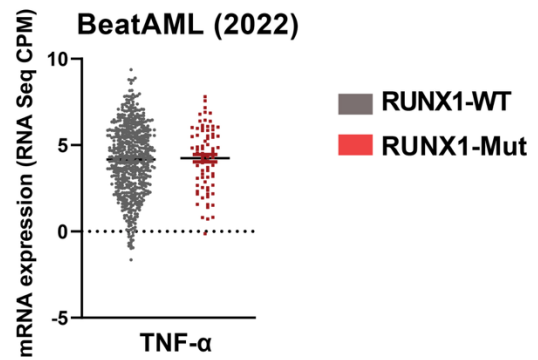


**Figure S1: TNFR2 (TNFRSF1B) is upregulated in *RUNX1*-mutated AML samples.** Using BeatAML databases, the expression of TNF- $\alpha$  and its receptors was evaluated among patient samples with (n=75) and without (n=560) *RUNX1* mutations using RNAseq data analysis. Panel **A** is the TNF- $\alpha$  receptors data from BeatAML 2022, and panel **B** is TNF- $\alpha$  expression. *P*-value significance was determined using an unpaired t-test between the unaffected and affected groups as \*\*\*  $p \leq 0.001$ .

## Supplemental Figure 2

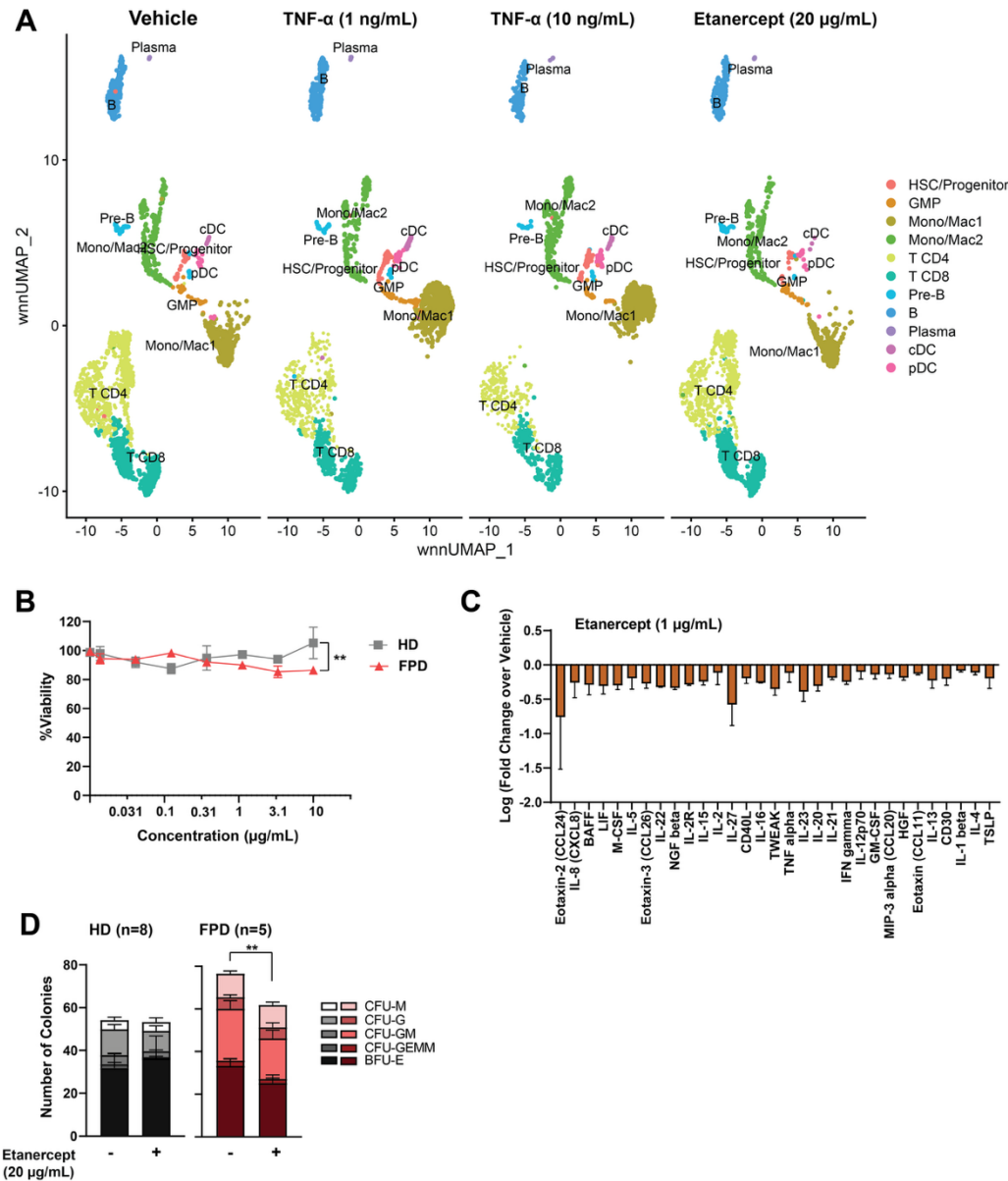


**Figure S2: Etanercept treatment can reverse *RUNX1*-FPD phenotype without causing toxicity.** **A**) *RUNX1*-FPD (n=2) bone marrow cells were cultured in IMDM medium supplemented with 20% FBS, 2mM L-glutamine, and 100U/mL penicillin-streptomycin, and treated overnight with TNF- $\alpha$  (1 ng/mL and 10ng/mL) and etanercept (20  $\mu$ g/mL). Cells then were subjected to 10x chromium single cell RNA sequencing. FASTQ files for the CITE-seq libraries were aligned to the human genome (GRCh38) on Cell Ranger v7.1.0 (10x Genomics), and the feature-barcode matrices were analyzed using Seurat v5. Approximately 2,600 cells in the vehicle, 2,200 cells in TNF- $\alpha$  (1 ng/mL), 1,700 cells in TNF- $\alpha$  (10 ng/mL), and 2,100 cells in the etanercept-treated groups were analyzed. The UMAP illustrates the clustering of different cell populations within each treatment group. **B**) The viability of FPD and HD MNCs was measured using MTS assay at 6 days post culture in the presence of etanercept at different concentrations. The assay was

performed in triplicate for each concentration. **C)** The cultured media from FPD MNCs (n=2) treated with etanercept (1 µg/mL) and vehicle were collected 48 hrs post-treatment. A 65-plex Luminex assay was performed to measure cytokine levels. The bar graph shows the log of fold changes in etanercept treatment over vehicle. **D)** The results of colony formation ability of FPD (n=5) and HD (n=8) CD34<sup>+</sup> HSPCs in the presence of etanercept. Primary CD34<sup>+</sup> cells were seeded at a density of 1,000 cells/well (in duplicate plating) and treated with etanercept at 20 µg/mL in MethoCult (*StemCell*, H4434). Colonies were counted on day 14 post-seeding.